Monthly Notices
of the
ROYAL ASTRONOMICAL SOCIETY

MNRAS **479,** L45–L49 (2018)
Advance Access publication 2018 June 01

doi:10.1093/mnrasl/sly096

Constraining the geometry of AGN outflows with reflection spectroscopy

M. L. Parker,[1]★ D. J. K. Buisson,[2] J. Jiang(姜嘉陈),[2] L. C. Gallo,[3] E. Kara,[4] G. A. Matzeu[1] and D. J. Walton[2]

[1]*European Space Agency (ESA), European Space Astronomy Centre (ESAC), Villanueva de la Cañada, E-28691 Madrid, Spain*
[2]*Institute of Astronomy, University of Cambridge, Madingley Road, CB3 0HA Cambridge, UK*
[3]*Saint Mary's University, Department of Astronomy & Physics, 923 Robie Street, Halifax, NS B3H 3C3, Canada*
[4]*Department of Astronomy, University of Maryland, College Park, MD 20742, USA*

Accepted 2018 May 29. Received 2018 May 18; in original form 2018 April 29

ABSTRACT

We collate active galactic nuclei (AGN) with reported detections of both relativistic reflection and ultrafast outflows. By comparing the inclination of the inner disc from reflection with the line-of-sight velocity of the outflow, we show that it is possible to meaningfully constrain the geometry of the absorbing material. We find a clear relation between the velocity and inclination, and demonstrate that it can potentially be explained either by simple wind geometries or by absorption from the disc surface. Due to systematic errors and a shortage of high-quality simultaneous measurements our conclusions are tentative, but this study represents a proof-of-concept that has a great potential.

Key words: accretion, accretion discs – black hole physics – galaxies: active.

1 INTRODUCTION

There are two main forms of relativistic spectroscopy in X-ray studies of active galactic nuclei (AGN): relativistic reflection and ultrafast outflows. Both rely on detecting red and blue-shifted elemental emission or absorption lines, usually from iron, and both reach velocities of a significant fraction of c. These two techniques are rarely used together, so the opportunities afforded by combining the two remain largely unexplored.

Relativistic reflection occurs when relatively cool, dense material in the accretion disc around a black hole is illuminated by X-rays. A featureless X-ray continuum is reprocessed into a series of fluorescent emission lines, absorption edges, and a Compton scattered hump (George & Fabian 1991). This characteristic reflection spectrum is then blurred and shifted by a combination of Doppler shifting, special relativistic boosting, and gravitational redshift (Fabian et al. 1989). By measuring the extent of these relativistic effects on the profile of the Fe K α line (or other lines, e.g. Fabian et al. 2009; Madej et al. 2014), we can infer physical parameters of the black hole and accretion disc, such as the inclination of the disc and the black hole spin parameter (see review by Reynolds 2014).

Ultrafast outflows (UFOs) are identified by strongly blueshifted absorption lines in X-ray spectra (Chartas et al. 2002; Pounds et al. 2003). They are generally thought to be due to winds from the AGN disc, accelerated by magnetic or radiation pressure (Reeves, O'Brien & Ward 2003; Fukumura et al. 2015), and are one possibility for driving an AGN feedback (e.g. Fabian 2012). An alternative possibility for producing these features is in an absorbing layer on the surface of the disc (Gallo & Fabian 2011, 2013), where the extreme velocity arises from the orbital motion of the gas and the absorption is imprinted on the reflection spectrum. Because we only have one line of sight (LOS) through the gas, it is extremely hard to directly measure the density and hence location of the absorbing material, so we must use other approaches to try and constrain the geometry of the gas.

While there is no reason to expect viewing angle to be the sole determiner of the LOS velocity, it should certainly have an impact, which depends on the launching mechanism. Radiation pressure-driven disc winds are expected to have an equatorial geometry (e.g. Proga, Stone & Kallman 2000), so velocity would generally increase with inclination, whereas magnetohydrodynamic (MHD) wind simulations predict higher velocities at low inclinations (Fukumura et al. 2010). In this work, we examine the possibility of constraining the geometry of UFOs using their inclination dependence, taking the inclination values from reflection modelling.

2 SAMPLE

We performed a literature search to identify sources that have both absorption from an outflow with a well-constrained velocity and a well-constrained inclination from relativistic reflection spectroscopy. In a few cases (Tombesi et al. 2011a; Parker et al. 2017, Parker et al., submitted) both are measured simultaneously, but for the majority these measurements are taken from different papers. In general, we prioritize results from papers presenting spectral fitting of an individual source over those where a large sample of sources are analysed. We also prefer more recent papers, as these are likely to have higher quality data sets available, as well as the

★ E-mail: mparker@sciops.esa.int

latest models. The selection of UFO and reflection results is presented in detail below, and the values are given in Table 1. The data and code used for the analysis in Section 3 are available at: https://github.com/M-L-Parker/UFO_inclinations.

2.1 UFOs

To avoid contamination from warm absorbers, we implement a velocity cut-off at $0.033c$ (10 000 km s^{-1}; Tombesi et al. 2010). These may or may not be related to UFOs (see discussion in e.g. Pounds & King 2013; Tombesi et al. 2013; Laha et al. 2016), and in general have small velocities or are consistent with the source rest frame (Laha et al. 2014).

The treatment of multiple detections must be carefully considered. We wish to avoid having the sample dominated by a small number of sources with multiple detections of the same outflow at different velocities. For example, the UFO in PDS 456 appears at slightly different velocities (from $\sim$0.23–0.33c) in almost every observation taken of the source (Gofford et al. 2014), most likely due to a flux-dependent velocity shift (Matzeu et al. 2017). However, an additional layer of ultrafast absorption is present in PDS 456 (Reeves et al. 2018b) simultaneously, which should be included separately. This is further complicated by the transient behaviour of outflowing absorption lines (e.g. Cappi et al. 2009), which is likely due to the gas being fully ionized at high source fluxes (Pinto et al. 2018) and inhomogeneities in the wind. To mitigate this, we combine multiple UFO detections from a single source into an averaged value when the velocity estimates are within the reported errors of each other, within $0.01c$ of each other, or within 10 per cent of each other, whichever is largest. Where the same authors have written multiple papers on a particular source, taking multiple velocity measurements, we assume that the later papers supersede earlier ones, and only use the latest values unless the outflows presented are clearly distinct. Otherwise, we include all values in our analysis.

2.2 Relativistic reflection

Obtaining a corresponding set of reflection measurements is simpler than the UFO case, as there should only be one value of the inclination for each AGN. We take the latest available measurement for each source, unless there is an earlier *NuSTAR* paper, in which case we use that value (in general, *NuSTAR*'s high energy coverage gives a better constraint on the reflection spectrum than soft instruments).

Reynolds (2014) gives a list of 'quality control' criteria for AGN spin measurements based on reflection spectroscopy. In brief, Reynolds suggests that a full ionized reflection model must be used; the iron abundance must be a free parameter; the inclination parameter must be free, and constrained; and the emissivity index must be free to vary and physically plausible. For the sake of keeping as large a sample as possible, we do not implement these as a strict requirement. Rather, we select all sources with a constrained inclination and flag those that do not meet these criteria. Then, in Section 3, we run the analysis on the full sample and on those results that meet the quality control criteria.

Where the errors on the inclination are less than 5°, we make the conservative assumption that the true uncertainty is dominated by systematic errors of $\pm5°$ (see e.g. the difference between RELXILL and REFLIONX discussed in Middleton et al. 2016). This applies in most cases. Finally, we exclude sources that require retrograde spin or significant disk truncation. In this case it is likely that the line is dominated by a narrow core, so the parameters are not reliable. The observed inclinations are strongly concentrated at 40–50°, which is most likely due to selection effects. At higher inclinations, the LOS is likely to intersect the torus, obscuring the nucleus, and at lower inclinations the relativistic blurring is weaker and correspondingly harder to measure.

3 RESULTS

3.1 Correlation analysis

We show the UFO velocity against reflection inclination points in Figs 1 and 3, overplotted with simple models (see Section 3.2). We use a Monte-Carlo approach to estimate the significance of any correlation between the two parameters. The distributions of v and i are approximately lognormal and normal, respectively, so we randomly draw 100 000 sets of points from distributions with the same mean and standard deviation [Mean $\log(v) = -0.89$, $\sigma_{\log(v)} = 0.29$, mean $i = 44.4$, $\sigma_i = 9.53$]. Of these simulated sets of points, we find 37 that exceed the Pearson correlation coefficient of the real data (0.64) and 629 that exceed the Spearman correlation coefficient (0.52). This gives probabilities of 0.0004 and 0.006 for a correlation this strong occurring from randomly distributed points. Excluding the two sources where the reflection modelling does not meet the Reynolds (2014) criteria marginally strengthens the correlation (Pearson $r = 0.63$, $P = 0.0011$, Spearman $r = 0.49$, $P = 0.017$).

3.2 Models

Regardless of whether a linear correlation is a significant improvement over the null hypothesis of randomly distributed points, it is still possible to use these points to infer something about the geometry of UFOs. We construct a simple imitation of a streamline, where a thin outflow starts moving vertically from the disc at some radius $r_{\rm launch}$, following a circular path with radius $r_{\rm curve}$. For this purpose, the units of radius are arbitrary. Once it reaches a final inclination $i_{\rm final}$ it leaves the circular path and travels on the tangent with $i = i_{\rm final}$. We also assume that the UFO accelerates along this path, following $v = v_{\rm inf}(1 - R_v/(R_v + r))^{\beta}$ (adapted from Knigge, Woods & Drew 1995; Sim et al. 2008), where β is a constant (and $\beta = 0$ gives a constant velocity) and R_v is a characteristic length-scale. We assume that the X-ray source is coincident with the black hole ($h = 0$, $r = 0$), and ignore all relativistic effects. This geometry is shown in Fig. 2. This geometry is intended as an approximation of that in radiation-driven winds (e.g. Proga et al. 2000), as these give a simple explanation for the higher velocities at higher inclinations. MHD winds predict concave streamlines (Fukumura et al. 2010), so give higher velocities at small inclinations. However, the exact pattern observed depends on the ionization and density structure within the wind, so it may still be possible to explain these results in an MHD scenario.

In most cases where the LOS intersects the wind in this model, it crosses the wind twice. Once while the wind is rising steeply, and once in the tail where the gradient is constant. Because of the radial acceleration assumed and close alignment with the LOS in the tail, this intersection results in a much higher apparent velocity. A simple way of only producing one measurable value for the velocity is to assume that the gas where the first intersection with the LOS occurs is fully ionized. In this case, no absorption lines would be produced, and only the second intersection would be observed. An example that provides a reasonable match to the data is shown in Fig. 1, with parameters $r_{\rm launch} = 10$, $r_{\rm curve} = 300$, $v_{\rm inf} = 0.5c$, and $R_v = 1000$. We show the effect of varying the acceleration coefficient β and final

Table 1. Outflow velocities and inclinations for the sources in our sample. Velocities with multiple references are the result of taking the weighted average of multiple measurements that meet the criteria discussed in Section 2.1. Similarly, sources with multiple velocities are those where multiple measurements did not meet the criteria for merging.

Name	$v_{\rm UFO}$ (c)	Reference	i (°)	Reference
1H 0419-577	0.079 ± 0.007	Tombesi et al. (2011b)	$49.0^{+7.0}_{-4.0}$	Walton et al. (2013)
1H 0707-495‡	$0.11^{+0.01}_{-0.02}$	Dauser et al. (2012)	43.0 ± 2.0	Kara et al. (2015)
	0.18 ± 0.01	Hagino et al. (2016); Dauser et al. (2012)		
3C 111‡	0.105 ± 0.006	Gofford et al. (2013); Tombesi et al. (2011a)	44.0 ± 2.0	Tombesi et al. (2011a)†
Ark 120	0.29 ± 0.02	Tombesi et al. (2011b)	$45.0^{+5.0}_{-2.0}$	García et al. (2014)
IC 4329A	0.098 ± 0.004	Tombesi et al. (2011b)	35.0 ± 5.0	Mantovani, Nandra & Ponti (2014)†
IRAS 00521-7054‡	$0.403^{+0.007}_{-0.006}$	Walton et al. (in prep)	63^{+3}_{-2}	Walton et al. (in prep)
IRAS 13224-3809‡	0.236 ± 0.006	Parker et al. (2017)	59.0 ± 1.0	Parker et al. (2017)
IRAS 13349+2438‡	0.13 ± 0.01	Parker et al. (submitted)	$48.0^{+2.0}_{-1.0}$	Parker et al. (submitted)
MCG-5-23-16	0.116 ± 0.004	Tombesi et al. (2011b)	51.0 ± 7.0	Zoghbi et al. (2017)
MR 2251-178	0.137 ± 0.008	Gofford et al. (2013)	$24.0^{+3.0}_{-5.0}$	Nardini et al. (2014)
Mrk 1044‡	0.10 ± 0.01	Mallick et al. (2018)	47 ± 3	Mallick et al. (submitted)
Mrk 509	0.14 ± 0.0024	Cappi et al. (2009); Tombesi et al. (2011b)	$50.0^{+5.0}_{-3.0}$	Walton et al. (2013)
	0.171 ± 0.003	Cappi et al. (2009); Tombesi et al. (2011b)		
	0.197 ± 0.005	Cappi et al. (2009); Tombesi et al. (2011b)		
Mrk 766	0.039 ± 0.03	Gofford et al. (2013)	$39.0^{+6.0}_{-3.0}$	Buisson et al. (submitted)
	0.082 ± 0.006	Tombesi et al. (2011b)		
Mrk 79	0.092 ± 0.004	Tombesi et al. (2011b)	24.0 ± 1.0	Gallo et al. (2011)
Mrk 841	0.055 ± 0.025	Tombesi et al. (2011b)	$46.0^{+6.0}_{-5.0}$	Walton et al. (2013)
NGC 4051	0.202 ± 0.006	Tombesi et al. (2011b)	37.0 ± 5.0	Risaliti et al.(in prep)
NGC 4151	0.0452 ± 0.0099	Gofford et al. (2013); Patrick et al. (2012)	<10	Beuchert et al. (2017)
	0.106 ± 0.007	Tombesi et al. (2011b)		
NGC 5506	0.246 ± 0.006	Gofford et al. (2013)	$41.0^{+0.1}_{-0.2}$	Sun et al. (2017)
PDS 456‡	0.278 ± 0.003	Reeves et al. (2018b); Matzeu et al. (2017)	65.0 ± 2.0	Chiang et al. (2017)
	0.46 ± 0.02	Reeves et al. (2018b)		
PG 1211+143‡	0.0598 ± 0.00069	Pounds et al. (2016); Danehkar et al. (2018); Reeves, Lobban & Pounds (2018a)	44.0 ± 2.0	Lobban et al. (2016)
	0.129 ± 0.002	Pounds et al. (2016)		
	0.151 ± 0.003	Tombesi et al. (2011b)		
Swift J2127	0.231 ± 0.006	Gofford et al. (2013)	49.0 ± 2.0	Marinucci et al. (2014)

†These results do not meet the quality control criteria of Reynolds (2014).
‡These sources have joint reflection/UFO fitting, which either gives the result reported here or is consistent with it.

inclination $i_{\rm final}$. From this it is clear that meaningful constraints on these parameters can be obtained.

An alternative way of giving a relation between the velocity of the absorption line and the viewing angle is to produce the absorption in the disc itself. This model, explored by Gallo & Fabian (2011, 2013), explains UFO absorption using a surface layer on the disc, with the strong blueshift due to the orbital velocity of the absorbing material, rather than an outflowing wind. In this case, the inclination dependence of the absorption velocity arises from the increased LOS velocity of the disc at high inclinations.

As a simple proxy for the velocity of an absorption line from the surface of the disc, we take the maximum blueshift from the RELLINE model (Dauser et al. 2010). This gives a simple correlation between i and v (shown in Fig. 3), although it does not reach high enough velocities to account for the most blueshifted absorption lines. The only parameter of this model is the black hole spin (a), but this has a limited effect as the maximum blueshift of the disc comes from further out than the innermost stable circular orbit. We note that this predicted velocity should be an upper limit as it is the maximum found on the disc, so points should generally lie below the line.

4 DISCUSSION

We note that there are other possible explanations for broad emission lines in AGN. For example, Nardini et al. (2015) interpret the emission line in PDS 456 as a P-Cygni profile, where the Fe K emission is produced by scattering off the outflowing wind. In this case, the relativistic broadening is produced by the velocity of the wind instead of the orbits in the disc (Done et al. 2007). This model relies on partial-covering absorption to explain most of the spectral complexity. However, Chiang et al. (2017) present an alternative model where the broad-band spectrum can be fully explained by relativistic reflection, warm absorption, and the UFO. This interpretation is supported by the detection of a soft X-ray lag, generally interpreted as reverberation in the inner disc and found in many unobscured sources (De Marco et al. 2013). While the detection of an X-ray lag is usually considered strong evidence for the presence of relativistic reflection in a source (and many of the sources in our sample show reverberation lags, Kara et al. 2016; De Marco et al. 2013), it is difficult to rule out a contribution to the total broad-line profile from scattering in the wind. Indeed, given that disc winds are likely to be most dense at the point where they launch from the disc and should be corotating with it, then scattering from the disc surface and wind may be thought of as a single continuous process. The impact of having Fe K emission from both the disc

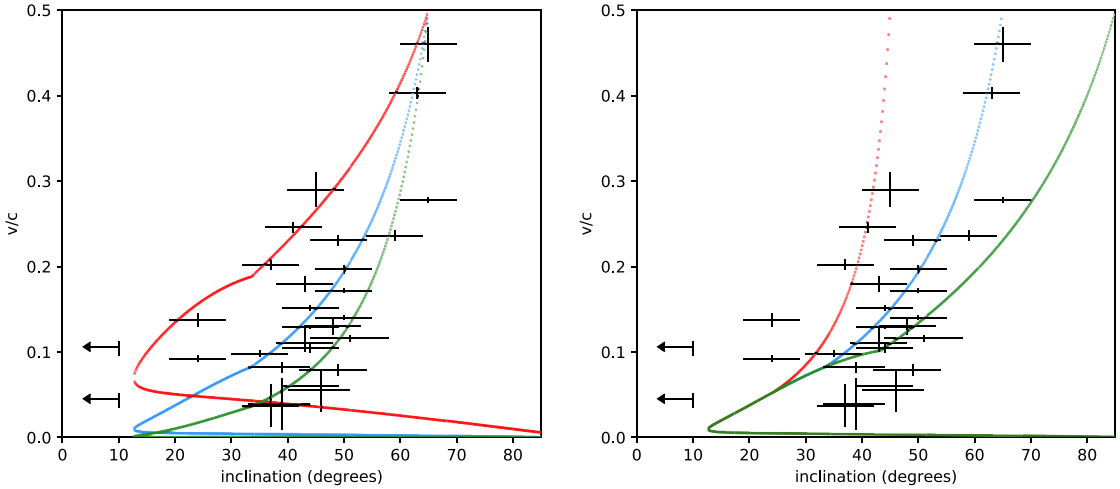

Figure 1. UFO velocity as a function of reflection inclination, overplotted with a toy model for an outflowing disc wind. Left: the effect of changing the acceleration coefficient β to 0.5 (red, left), 1.0 (blue, middle) and 1.5 (green, right) with final inclination $i_{\rm final} = 65^\circ$. Right: the effect of setting $i_{\rm final}$ to 45° (red, left), 65° (blue, middle), and 85° (green, right) with $\beta = 1$.

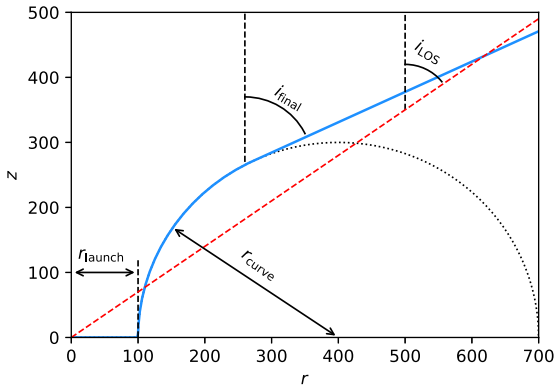

Figure 2. Simple streamline geometry, with the wind shown in blue and the LOS in red (dashed). Length units are arbitrary.

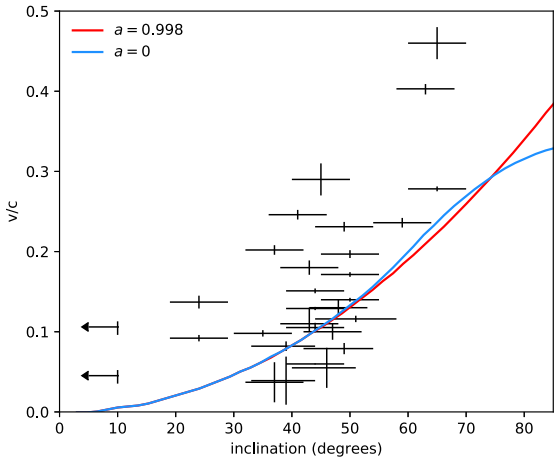

Figure 3. Toy model for absorption from a layer on the disc.

and wind is not understood, but could have a significant effect on the measured inclination. A higher velocity outflow will produce more blueshifted emission, in the same way that a higher inclination gives a more blueshifted line profile for disc reflection. We note that the tentative relation identified here may be indicative of the effect of wind emission on the net relativistic line profile rather than an inclination dependence. A related issue is the lack of simultaneous UFO/reflection modelling. Using a simplified phenomenological continuum may exaggerate the significance of line features, leading to false detections (Zoghbi et al. 2015). Similarly, not accounting for UFO absorption during reflection modelling may bias the measured parameters. We will revisit the spectra of some of these sources for joint modelling to investigate this further in future work.

We have assumed throughout that all UFOs have the same shape and velocity profile, and that the observed velocity is solely determined by the LOS angle. This is unlikely to be the case in practice: the accretion rate, for example, is likely to have a major impact on the velocity of the material. Similarly, we have implicitly assumed that wind instabilities play a negligible role in determining the observed velocity, which is unlikely. Another caveat is that our sample is anything but unbiased, and the biases are poorly understood. Reflection measurements are generally biased towards high spin (Vasudevan et al. 2016), and there may be a similar bias towards high inclination, as it produces broader, easier to measure lines. Similarly, it is plausible that UFO velocity measurements are biased towards lower velocities, as the sensitivity of X-ray detectors typically declines with energy (although this may be remedied as the *NuSTAR* archive grows).

5 CONCLUSIONS

We have identified a correlation between the velocity of highly ionized absorption features from UFOs and the inclination of the inner accretion disc measured from reflection spectroscopy. The correlation is formally significant, but heavily reliant on a small number of points at high velocity.

We show that the observed points can be explained by simple toy models of an outflowing wind or absorption from a disc, although the latter cannot account for the highest velocity features. With more detailed modelling and higher quality data, this technique could be very powerful for constraining the geometry of outflowing material in AGN.

ACKNOWLEDGEMENTS

MLP and GAM are supported by European Space Agency(ESA) Research Fellowships. JJ acknowledges support by the Cambridge Trust and the Chinese Scholarship Council Joint Scholarship Programme (201604100032). DJKB is supported by an STFC studentship.

REFERENCES

Beuchert T. et al., 2017, A&A, 603, A50
Cappi M. et al., 2009, A&A, 504, 401
Chartas G., Brandt W. N., Gallagher S. C., Garmire G. P., 2002, ApJ, 579, 169
Chiang C.-Y., Cackett E. M., Zoghbi A., Fabian A. C., Kara E., Parker M. L., Reynolds C. S., Walton D. J., , 2017, MNRAS, 472, 1473
Danehkar A. et al., 2018, ApJ, 853, 165
Dauser T. et al., 2012, MNRAS, 422, 1914
Dauser T., Wilms J., Reynolds C. S., Brenneman L. W., 2010, MNRAS, 409, 1534
De Marco B. et al., 2013, MNRAS, 431, 2441
Done C., Sobolewska M. A., Gierliński M., Schurch N. J., 2007, MNRAS, 374, L15
Fabian A. C. et al., 2009, Nature, 459, 540
Fabian A. C., 2012, ARA&A, 50, 455
Fabian A. C., Rees M. J., Stella L., White N. E., 1989, MNRAS, 238, 729
Fukumura K., Kazanas D., Contopoulos I., Behar E., 2010, ApJ, 715, 636
Fukumura K., Tombesi F., Kazanas D., Shrader C., Behar E., Contopoulos I., 2015, ApJ, 805, 17
Gallo L. C., Miniutti G., Miller J. M., Brenneman L. W., Fabian A. C., Guainazzi M., Reynolds C. S., 2011, MNRAS, 411, 607
Gallo L. C., Fabian A. C., 2011, MNRAS, 418, L59
Gallo L. C., Fabian A. C., 2013, MNRAS, 434, L66
García J. et al., 2014, ApJ, 782, 76
George I. M., Fabian A. C., 1991, MNRAS, 249, 352
Gofford J., Reeves J. N., Tombesi F., Braito V., Turner T. J., Miller L., Cappi M., 2013, MNRAS, 430, 60
Gofford J. et al., 2014, ApJ, 784, 77
Hagino K., Odaka H., Done C., Tomaru R., Watanabe S., Takahashi T., 2016, MNRAS, 461, 3954
Kara E. et al., 2015, MNRAS, 449, 234
Kara E., Alston W. N., Fabian A. C., Cackett E. M., Uttley P., Reynolds C. S., Zoghbi A., 2016, MNRAS, 462, 511
Knigge C., Woods J. A., Drew J. E., 1995, MNRAS, 273, 225
Laha S., Guainazzi M., Dewangan G. C., Chakravorty S., Kembhavi A. K., 2014, MNRAS, 441, 2613
Laha S., Guainazzi M., Chakravorty S., Dewangan G. C., Kembhavi A. K., 2016, MNRAS, 457, 3896
Lobban A. P., Pounds K., Vaughan S., Reeves J. N., 2016, ApJ, 831, 201
Madej O. K., Garcia J., Jonker P. G., Parker M. L., Ross R., Fabian A. C., Chenevez J., 2014, MNRAS, 442, 1157
Mantovani G., Nandra K., Ponti G., 2014, MNRAS, 442, L95
Marinucci A. et al., 2014, MNRAS, 440, 2347
Matzeu G. A., Reeves J. N., Braito V., Nardini E., McLaughlin D. E., Lobban A. P., Tombesi F., Costa M. T., 2017, MNRAS, 472, L15
Middleton M. J., Parker M. L., Reynolds C. S., Fabian A. C., Lohfink A. M., 2016, MNRAS, 457, 1568
Nardini E. et al., 2015, Science, 347, 860
Nardini E., Reeves J. N., Porquet D., Braito V., Grosso N., Gofford J., 2014, MNRAS, 440, 1200
Parker M. L. et al., 2017, Nature, 543, 83
Patrick A. R., Reeves J. N., Porquet D., Markowitz A. G., Braito V., Lobban A. P., 2012, MNRAS, 426, 2522
Pinto C. et al., 2018, MNRAS, 476, 1021
Pounds K. A., King A. R., 2013, MNRAS, 433, 1369
Pounds K. A., Reeves J. N., Page K. L., Wynn G. A., O'Brien P. T., 2003, MNRAS, 342, 1147
Pounds K., Lobban A., Reeves J., Vaughan S., 2016, MNRAS, 457, 2951
Proga D., Stone J. M., Kallman T. R., 2000, ApJ, 543, 686
Reeves J. N., O'Brien P. T., Ward M. J., 2003, ApJ, 593, L65
Reeves J. N., Lobban A., Pounds K. A., 2018a, ApJ, 854, 28
Reeves J. N., Braito V., Nardini E., Lobban A. P., Matzeu G. A., Costa M. T., 2018b, ApJ, 854, L8
Reynolds C. S., 2014, Space Sci. Rev., 183, 277
Sim S. A., Long K. S., Miller L., Turner T. J., 2008, MNRAS, 388, 611
Sun S. et al., 2018, MNRAS, 478, 1900
Tombesi F., Cappi M., Reeves J. N., Palumbo G. G. C., Yaqoob T., Braito V., Dadina M., 2010, A&A, 521, A57
Tombesi F., Cappi M., Reeves J. N., Nemmen R. S., Braito V., Gaspari M., Reynolds C. S., 2013, MNRAS, 430, 1102
Tombesi F., Sambruna R. M., Reeves J. N., Reynolds C. S., Braito V., 2011a, MNRAS, 418, L89
Tombesi F., Cappi M., Reeves J. N., Palumbo G. G. C., Braito V., Dadina M., 2011b, ApJ, 742, 44
Vasudevan R. V., Fabian A. C., Reynolds C. S., Aird J., Dauser T., Gallo L. C., 2016, MNRAS, 458, 2012
Walton D. J., Nardini E., Fabian A. C., Gallo L. C., Reis R. C., 2013, MNRAS, 428, 2901
Zoghbi A. et al., 2015, ApJ, 799, L24
Zoghbi A. et al., 2017, ApJ, 836, 2

This paper has been typeset from a TEX/LATEX file prepared by the author.